Heuristic Optimization of PI Controllers for Time-Delayed LFC-EV Systems

Ömer AYDIN[1], Suud Ademnur HASEN[2], and Saffet AYASUN[2]

[1]Department of Electrical and Electronics Engineering, Erzincan Binali Yıldırım University, Erzincan, Türkiye
oaydin@erzincan.edu.tr
[2]Department of Electrical and Electronics Engineering, Gazi University, Ankara, Türkiye
suudademnur.hasen@gazi.edu.tr, saffetayasun@gazi.edu.tr

Abstract

This study proposes an optimization method for the proportional–integral (PI) controller gains of a single-area time-delayed load frequency control system with electric vehicles (LFC-EV). Four heuristic algorithms are used to optimize the PI controller gains: crow search algorithm (CSA), particle swarm optimization (PSO), vortex search algorithm (VSA), and sine-cosine algorithm (SCA). The integral square error (ISE) objective function is used in the optimization process for all algorithms. Finally, a time-domain simulation of the LFC-EV system is conducted to evaluate the performance of the proposed algorithms. The optimized PI controller gains exhibited superior performance compared to randomly selected gains, leading to decreased oscillations and faster settling times, as evidenced by the results.

1. Introduction

The use of renewable energy sources (RESs) has an important place in modern power systems. While increasing the use of RESs has environmental and financial benefits, it can also pose challenges for frequency control due to the uncertainty of RES generation [1]. This element has led to an increase in the significance of LFC systems, which control the frequency of power systems.

Since LFC systems are essential for the stability and safety of power systems, researchers are looking for ways to make them faster and more reliable. This has led to the exploration of using auxiliary services such as demand response, EVs, fuel cells, and virtual inertia in LFC systems [2-5]. These auxiliary services and the remote points of the power system need to communicate with the controller, and the controller relies on communication systems to transmit control signals. This introduces additional challenges, as current technology does not allow for instantaneous reception of information signals, processing of information, and transmission of control signals to the relevant unit. Therefore, the inevitability of time delays in the control stages of LFC systems highlights the need to consider time delays in stability analysis [6].

Due to the negative impact of unavoidable time delays on power system stability and safety, there has been a growing interest in studies that consider time delays [7-11]. The stability delay margins obtained for LFC systems provide important insights into system stability. Some studies have also investigated obtaining robust stability regions of LFC systems [12-15]. The robust stability regions obtained in these studies contain the controller gain sets that ensure the stable operation of the relevant system. This means that the system is stable for any set of controllers selected within the robust stability region.

Heuristic algorithms are the most effective way to find the best controller gain set. These algorithms work by first generating candidate controller gains and then iteratively determining the best set. In recent years, there has been a growing body of research on the optimization of controller gains using heuristic algorithms. A study in [16] used teaching learning based optimization to analyze the performance of automatic LFC in multi-source power systems. Another study in [17] proposed a bacteria foraging optimization algorithm based LFC system to suppress oscillations in power systems. Artificial bee colony algorithm was proposed in [18] to optimize the proportional–integral–derivative (PID) controller gains of the LFC system. In [19], the authors employed the bat algorithm to optimize the PI controller gains for the LFC systems of interconnected power systems. A hybrid algorithm consisting of harmony search and cuckoo optimization algorithm was proposed in [20] to design a controller for LFC systems. In [21], the authors proposed a PID controller based on tribe-de optimization algorithm and rule weight adjustment method for the LFC systems of multi-area power systems. In [22], the LFC problem in two-area non-reheated thermal power system, multi-units hydro thermal system, multi-sources system, and three unequal area power system equipped with PI and PID controller was solved using grey wolf optimization algorithm.

Most studies in the literature optimize the algorithm parameters for a specific system. Additionally, to the knowledge of the authors, none of the previous heuristic optimization studies have considered a system that directly uses EVs in LFC system. This study investigates the optimization of PI controller gains using the CSA, PSO, VSA, and SCA in a time-delayed LFC-EV system, where EVs are used as an auxiliary service for LFC. To provide more accurate and clear performance comparisons of the algorithms, all studies are conducted on the same system with the same particle size and termination criteria.

The rest of the study is organized as follows: Section 2 presents the LFC-EV system model. Section 3 discusses the optimization techniques used to optimize the PI controller gains. Section 4 presents the results obtained, and Section 5 concludes the paper.

2. Time-Delayed Single-Area LFC-EV System

The PI controller is employed in the LFC-EV system depicted in Fig. 1. The time delay, modeled as $e^{-s\tau}$, affects both the conventional frequency control loop and the auxiliary EV service. The participation factors α_0 and α_1, which sum to one, determine the participation of the conventional system and the EV group in frequency control. $D, M, R, T_g, T_c, T_r, F_p, K_{EV}$, T_{EV}, and τ denote generator damping coefficient, generator moment of inertia, speed regulation coefficient, regulator time constant, reheat turbine time constant, total turbine power ratio, fraction of total turbine power, EV battery gain, EV battery time constant and time delay, respectively. The state space equation of the LFC-EV system can be expressed as follows [23]:

$$x(t) = A_0 x(t) + A_d x(t-\tau) + F\Delta P_L(t) \tag{1}$$

where, the state vector and system matrices in terms of system parameters are:

$$x(t) = \begin{bmatrix} \Delta f & \Delta P_g & \Delta P_m & \Delta X_g & \Delta P_{EV} & \int ACE \end{bmatrix}^T$$

$$ACE = \beta.\Delta f$$

$$A_0 = \begin{bmatrix} -\dfrac{D_i}{M_i} & -\dfrac{1}{M_i} & 0 & 0 & \dfrac{1}{M_i} & 0 \\ 0 & -\dfrac{1}{T_c} & \dfrac{1}{T_c} & 0 & 0 & 0 \\ -\dfrac{F_P}{T_{gi}R_i} & 0 & -\dfrac{1}{T_r} & \left(-\dfrac{1}{T_r} - \dfrac{F_P}{T_g}\right) & 0 & 0 \\ -\dfrac{1}{T_{gi}R_i} & 0 & 0 & -\dfrac{1}{T_{gi}} & 0 & 0 \\ 0 & 0 & 0 & 0 & -\dfrac{1}{T_{EV}} & 0 \\ \dfrac{\beta K_P D}{M} - \beta K_I & -\dfrac{\beta K_P}{M} & 0 & 0 & -\dfrac{\beta K_P}{M} & 0 \end{bmatrix}$$

$$A_d = \begin{bmatrix} 0 & 0 & 0 & 0 & 0 & 0 \\ 0 & 0 & 0 & 0 & 0 & 0 \\ 0 & 0 & 0 & 0 & 0 & \dfrac{F_P \alpha_0}{T_g} \\ 0 & 0 & 0 & 0 & 0 & \dfrac{\alpha_0}{T_g} \\ 0 & 0 & 0 & 0 & 0 & \dfrac{K_{EV}\alpha_1}{T_{EV}} \\ 0 & 0 & 0 & 0 & 0 & 0 \end{bmatrix}$$

To analyze the stability of the single-area LFC-EV system shown in Fig. 1, we first need to obtain the system's characteristic equation, which is written as follows:

$$\Delta(s,\tau) = P(s) + Q(s)e^{-s\tau} = 0 \tag{2}$$

where, the coefficients P and Q are polynomials expressed in the s plane, depending on the system parameters. The coefficients and degrees of these polynomials are given as:

$$\begin{aligned} P(s) &= p_6 s^6 + p_5 s^5 + p_4 s^4 + p_3 s^3 + p_2 s^2 + p_1 s^1 + p_0 \\ Q(s) &= q_4 s^4 + q_3 s^3 + q_2 s^2 + q_1 s^1 + q_0 \end{aligned} \tag{3}$$

The coefficients of the $P(s)$ and $Q(s)$ polynomials are determined as:

$$\begin{aligned}
p_6 &= MRT_g T_r T_c T_{EV} \\
p_5 &= DRT_g T_r T_c T_{EV} + MR(T_g T_r T_c + T_r T_c T_{EV} + T_g T_c T_{EV} + T_g T_r T_{EV}) \\
p_4 &= DR(T_g T_r T_c + T_r T_c T_{EV} + T_g T_c T_{EV} + T_g T_r T_{EV}) \\
&\quad + MR(T_r T_c + T_g T_c + T_g T_r + T_c T_{EV} + T_r T_{EV} + T_g T_{EV}) \\
p_3 &= DR(T_r T_c + T_g T_c + T_g T_r + T_c T_{EV} + T_r T_{EV} + T_g T_{EV}) + MR(T_c + T_r + T_g + T_{EV}) \\
&\quad + F_p T_r T_{EV} + K_P\left[a_0 \beta R F_p T_r T_{EV}\right] \\
p_2 &= DR(T_c + T_r + T_g + T_{EV}) + MR + F_p T_r + T_{EV} + K_P\left[a_0 \beta R\left(T_{EV} + F_p T_r\right)\right] \\
&\quad + K_I\left[a_0 \beta R F_p T_r T_{EV}\right] \\
p_1 &= DR + 1 + K_P\left[a_0 \beta R\right] + K_I\left[a_0 \beta R\left(T_{EV} + F_p T_r\right)\right] \\
p_0 &= K_I\left[a_0 \beta R\right] \\
q_4 &= K_P\left[a_1 \beta R K_{EV} T_g T_r T_c\right] \\
q_3 &= K_P\left[a_1 \beta R K_{EV}\left(T_r T_c + T_g T_c + T_g T_r\right)\right] + K_I\left[a_1 \beta R K_{EV} T_g T_r T_c\right] \\
q_2 &= K_P\left[a_1 \beta R K_{EV}\left(T_c + T_r + T_g\right)\right] \\
&\quad + K_I\left[a_1 \beta R K_{EV}\left(T_r T_c + T_g T_c + T_g T_r\right)\right] \\
q_1 &= K_P\left[a_1 \beta R K_{EV}\right] + K_I\left[a_1 \beta R K_{EV}\left(T_c + T_r + T_g\right)\right] \\
q_0 &= K_I\left[a_1 \beta R K_{EV}\right]
\end{aligned}$$

3. Optimization of PI Controllers

Optimization algorithms generally follow the same basic structure, but they differ in the mathematical search structures they use during optimization. First, the algorithms generate initial candidate solutions that satisfy the problem's constraints. Then, they iteratively evaluate the candidate solutions in the

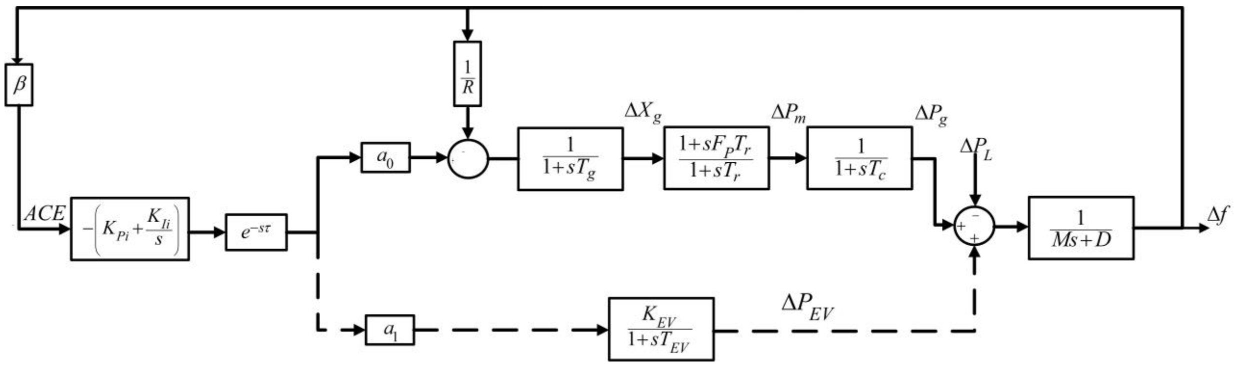

Fig. 1. Dynamic model of LFC-EV system

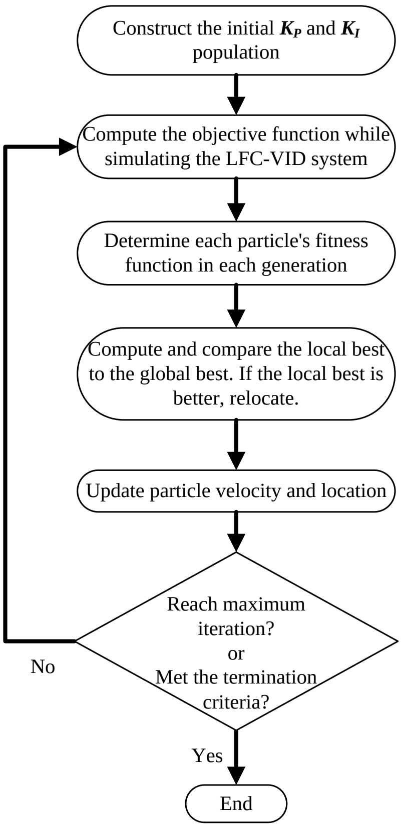

Fig. 2. PI controller gains optimization flowchart.

problem's objective function and assign a fitness value to each candidate solution. Based on the fitness values, the algorithms find the local and global best solutions and modify the search in the candidate solution space accordingly using certain mathematical operations. This study uses the ISE objective function for all algorithms to make the comparison of the algorithms more reliable [24].

$$ObjFunc = \int_0^T (\Delta f)^2 dt \tag{4}$$

The mathematics used in the search processes of optimization algorithms are often inspired by living things or natural phenomena. The CSA mimics the crows' memory and post-tracking food-thieving tactics. Each crow follows the previous crow and stores the location of the food in its memory. In the next stage, the crow uses this information to update its location and shift the search to a new area. This process is repeated iteratively until the best solution is found [25].

The PSO mimics the collective behavior of living things in security and foraging. The algorithm consists of a swarm of particles with initial positions and velocities. Individuals in the herd seek food separately, that is, in this case, a solution. Since each member of the swarm is in communication with each other, the best position obtained is recorded and in the next iteration, the positions and velocities of the particles are updated using this information. In this way, it tries to reach the best solution in the search space [26].

The VSA mimics the behavior of vortices in nature to find the best solution in the search space. Initially, the algorithm determines the diameter and center point of the initial vortex in the space of candidate solutions, considering the problem constraints. Then, it evaluates the candidate solutions in the vortex using the objective function and assigns a fitness value to each solution. Based on the fitness values, the algorithm determines the diameter of the vortex to be used in the next step, which should be smaller than the diameter of the previous vortex. The algorithm also shifts the center of the vortex to the point where the best solution has been found so far. By reducing the diameter of the vortex in each iteration, the algorithm reduces the size of the search space, which helps it to reach the best solution quickly and efficiently [27].

The SCA, like other algorithms, uses candidate solutions whose positions are determined at the beginning. However, instead of mimicking living things in nature, the SCA uses the sine and cosine functions to generate different scanning angles. The positions of the particles and the distance they move are determined by these functions. Additionally, the algorithm allows particles to transition between the sine and cosine functions, which expands the search region of each particle [28].

The flowchart in Fig. 2 illustrates how to use the algorithms to obtain the optimal PI controller gains for the LFC-EV system.

4. Results

This section presents the results of optimizing the PI controller gains for the LFC-EV system. The parameters of the single-area LFC-EV system are the same as in the reference study [23]. The sharing factors for the analysis are set to $a_0 = 0.8$ and $a_1 = 0.2$. The time delay τ is chosen to be $0.5s$. To ensure a fair comparison, the particle size and maximum iteration number of all algorithms were set to 50. The analyses were then carried out using these parameters.

Modern electrical networks have a frequency standard deviation of $0.2Hz$. This equates roughly to $0.004\,p.u.$ in a $50Hz$ network. In this study, the settling time of the frequency response is defined as the time it takes for the frequency to return to within $0.004\,p.u.$ of its nominal value.

To start the analysis, each algorithm is run with the PI controller gains search space range of [0,1] of the initial candidate solutions. Once the PI controller gains are obtained, they are used in time-domain simulations of the LFC-EV system to obtain a frequency response for each PI controller set. For each scenario, the performance specifications such as peak overshoot (OS), peak undershoot (US), and settling time (ST) is computed using the optimal PI controller gains obtained via the heuristic algorithms. The results are presented in Table I. In Fig. 3, the frequency responses specification of the LFC-EV system that were obtained using the optimal K_P and K_I gain values from each algorithm are displayed.

Table 1. Optimized PI controller gains and their corresponding frequency response specifications

	K_P	K_P	**US**	**OS**	**ST**
CSA	0.5182	0.0461	0.03659	0.001203	9.876
PSO	0.521	0.0449	0.03653	0.0008868	10.01
VSA	0.5312	0.0469	0.03615	0.001029	9.778
SCA	0.5205	0.0415	0.03665	0.0001959	10.46
Random	0.5	0.2	0.03396	0.02062	17.63

Overall, the results illustrate the US values are similar for all algorithms, with the VSA performing slightly better. However, the SCA algorithm is the best in terms of OS values. The CSA algorithm produces the gain values that result in the highest OS values. In terms of ST, the VSA algorithm gives the best results, while the SCA algorithm gives the worst results. Based on these results, it can be concluded that the VSA algorithm is a good choice for minimizing ST, while the SCA algorithm is a good choice for minimizing OS.

To demonstrate the effectiveness of the optimized PI controller gains, the frequency response of the LFC-EV system was obtained with randomly selected PI gains $(K_P = 0.5, K_I = 0.2)$. The optimized PI controller gain by the SCA algorithm manages to reduce the peak OS by $\approx 0.02042\,pu$ and settling time by $\approx 7.17s$ as presented in Table I and in Fig. 4. Hence, the frequency response obtained with the optimized PI controller gains is significantly better, with lower OS, US, and ST.

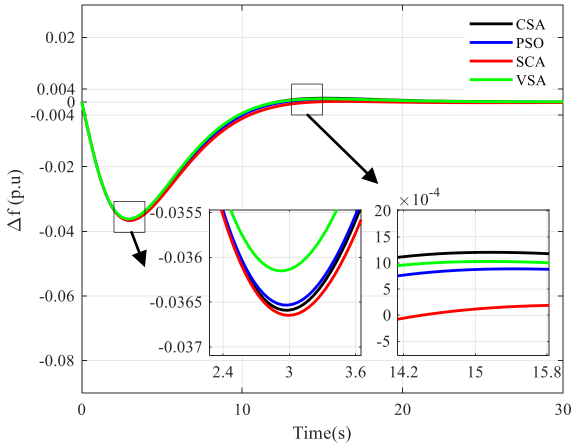

Fig. 3. Frequency response for optimal PI controller gains

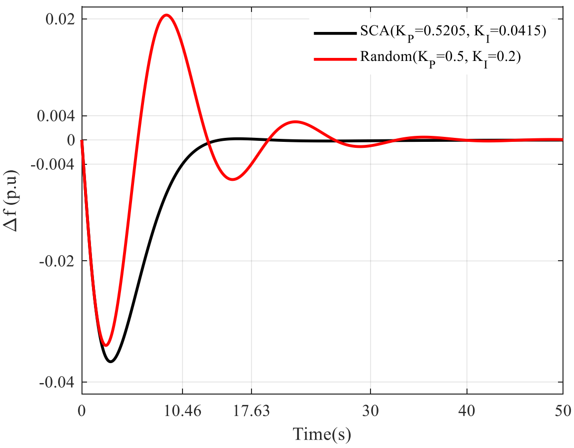

Fig. 4. Frequency response for random and SCA obtained PI controller gains.

5. Conclusions

This study aims to optimize the PI controller gains of an LFC-EV system to improve its frequency response characteristics, such as peak overshoot, undershoot, and settling time. Four optimization algorithms were used to compare their performance and to find the best PI controller gains. The results showed that the sine-cosine algorithm outperformed the other three algorithms in terms of peak overshoot optimization, while the vortex search algorithm outperformed the other three algorithms in terms of settling time optimization. Randomly selected PI controller gains resulted in significantly higher oscillations and longer settling time, demonstrating the superiority of the optimized PI controller gains.

6. References

[1] S. S. Dhillon, J. S. Lather, and S. Marwaha, "Multi objective load frequency control using hybrid bacterial foraging and particle swarm optimized PI controller," *Int. J. Electr. Power Energy Syst.*, vol. *79*, pp. *196-209*, Jan 2016.

[2] S. A. Pourmousavi, and M. H. Nehrir, "Real-time central demand response for primary frequency regulation in microgrids," *IEEE Trans. Smart Grid*, vol. *3*, no. *4*, pp. *1988-1996*, Jun 2012.

[3] N. Ausnain, Ş. Sönmez, and S. Ayasun, "Impact of electric vehicles aggregators with communication delays on stability delay margins of two-area load frequency control system." *Trans. Inst. Meas. Contr.*, vol. *43*, no. *12*, pp. *2860-2871*, Aug 2021.

[4] M. H. Özdemir, "The effects of the FOPI controller and time delay on stability region of the fuel cell microgrid." *Int. J. Hydrogen Energy*, vol. *45*, no. *60*, pp. *35064-35072*, Jul 2020.

[5] G. Delille, B. François, and G. Malarange., "Dynamic frequency control support: A virtual inertia provided by distributed energy storage to isolated power systems." *2010 IEEE PES Innovative Smart Grid Technologies Conference Europe (ISGT Europe)*, Gothenburg, Sweden, Nov 2010.

[6] Phadke, and G. Arun, "Synchronized phasor measurements in power systems," *IEEE Comput. Appl. Power*, vol. *6*, no. *2*, pp. *10-15*, Apr 1993.

[7] S. Ayasun and A. Gelen, "Stability analysis of a generator excitation control system with time delays," *Electr. Eng.*, vol. *91*, pp. *347-355*, Dec 2010.

[8] S. Ayasun, U. Eminollu, and Ş. Sönmez, "Computation of stability delay margin of time-delayed generator excitation control system with a stabilizing transformer," *Math. Problem. Eng.*, 392535, May 2014.

[9] K. Ramakrishnan, "Delay-dependent stability of networked generator-excitation control systems: an LMI based approach," *IFAC-Pap.*, vol. *49*, no. *1*, pp. *431-436*, Feb 2016.

[10] S. Liu, X. Wang, and P. X. Liu, "Impact of communication delays on secondary frequency control in an islanded microgrid," *IEEE Trans. Ind. Electron.*, vol. *62*, no. *4*, pp. *2021-2031*, Apr 2015.

[11] H. Erol, "Delay margin computation of generator excitation control system by using fractional order controller," *Trans. Inst. Meas. Contr.*, vol. *42*, no. *13*, pp. *2465–2474*, May 2020.

[12] A. K. Bhullar, R. Kaur, and S. Sondhi, "Modified neural network algorithm based robust design of AVR system using the Kharitonov theorem," *Int. J. Intell. Systems*, vol. *37*, no. *2*, pp. *1339-1370*, Nov 2022.

[13] S. Saxena, and Y. V. Hote, "Decentralized PID load frequency control for perturbed multi-area power systems,"

Int. J. Electr. Power Energy Syst., vol. *81*, pp. *405-415*, Mar 2016.

[14] J. Sharma, Y. V. Hote, and R. Prasad, "PID controller design for interval load frequency control system with communication time delay," *Control Eng. Pract*, vol. 89, pp. 154-168, Jun 2019.

[15] J. Sharma, Y. V. Hote, and R. Prasad, "Computation of parametric uncertainty margin using stability boundary locus: An application to load frequency control," *Trans. Inst. Meas. Control*, vol. *44*, no. *12*, pp. *2308-2322*, Aug 2022.

[16] A. K. Barisal, "Comparative performance analysis of teaching learning based optimization for automatic load frequency control of multi-source power systems," *Int. J. Electr. Power Energy Syst.*, vol. *66*, pp. *67-77*, Nov 2014.

[17] E. S. Ali, and S. M. Abd-Elazim, "Bacteria foraging optimization algorithm based load frequency controller for interconnected power system," *Int. J. Electr. Power Energy Syst.*, vol. *33*, no. *3*, pp. *633-638*, Jan 2011.

[18] M. Elsisi, M. Soliman, M. A. S. Aboelela, and W. Mansour, "ABC based design of PID controller for two area load frequency control with nonlinearities," *TELKOMNIKA Indonesian J. Electr.l Eng.*, vol. *16*, no. *1*, pp. *58-64*, Oct 2015.

[19] M. R. Sathya, and M. M. T. Ansari, "Load frequency control using Bat inspired algorithm based dual mode gain scheduling of PI controllers for interconnected power system," *Int. J. Electr. Power Energy Syst*., vol. *64*, pp. *365-374*, Aug 2014.

[20] M. Gheisarnejad, "An effective hybrid harmony search and cuckoo optimization algorithm based fuzzy PID controller for load frequency control," *Appl. Soft Comput.*, vol. *65*, pp. *121-138*, Jan 2018.

[21] N. Jalali, H. Razmi, and H. Doagou-Mojarrad, "Optimized fuzzy self-tuning PID controller design based on Tribe-DE optimization algorithm and rule weight adjustment method for load frequency control of interconnected multi-area power systems," *Appl. Soft Comput.*, vol. *93*, *106424*, May 2020.

[22] D. Guha, P. K. Roy, and S. Banerjee, "Load frequency control of interconnected power system using grey wolf optimization," *Swarm Evol*, vol. *27*, pp. *97-115*, Apr 2016.

[23] Ko, K. S., and Sung, D. K., "The effect of EV aggregators with time-varying delays on the stability of a load frequency control system," *IEEE Trans. Power Syst.*, vol *33*, no. *1*, pp. *669-680*, Apr 2017.

[24] T. S. Bhatti, A. A. F. Al-Ademi, and N. K. Bansal, "Load frequency control of isolated wind diesel hybrid power systems," *Energy Convers*, vol. *38*, no. *9*, pp. *829-837*, Jun 1997.

[25] A. Askarzadeh, "A novel metaheuristic method for solving constrained engineering optimization problems: crow search algorithm," *Comput Struct*, vol. *169*, pp. *1-12*, Mar 2016.

[26] J. Kennedy, and R. Eberhart, "Particle swarm optimization," *In Proceedings of ICNN'95-International Conference on Neural Networks*, Perth, Australia, Nov 1995.

[27] B. Doğan, and T. Ölmez, "A new metaheuristic for numerical function optimization: Vortex Search algorithm," *Inf. Sci*, vol. *293*, pp. *125-145*, Sep 2014.

[28] S. Mirjalili, "SCA: a sine cosine algorithm for solving optimization problems," *Knowl Based Syst*, vol. *96*, pp. *120-133*, Jan 2016.